Sol−Gel Synthesis of Vanadium Oxide within a Block Copolymer Matrix

Elsa A. Olivetti, Jong Hak Kim,† Donald R. Sadoway, Ayse Asatekin, and Anne M. Mayes*

Department of Materials Science and Engineering, Massachusetts Institute of Technology, Cambridge, Massachusetts 02139-4307

Received January 17, 2006. Revised Manuscript Received April 7, 2006

Films consisting of a vanadium pentoxide (i.e., V_2O_5) phase formed within a rubbery block copolymer were developed for their potential use as nanocomposite cathodes in lithium rechargeable batteries. Nanocomposite films were prepared by sol−gel synthesis from vanadyl triisopropoxide precursor in poly(oligooxyethylene methacrylate)-*block*-poly(butyl methacrylate), POEM-*b*-PBMA. The in situ growth of amorphous V_2O_5 was confirmed by wide-angle X-ray scattering (WAXS), X-ray photoelectron spectroscopy (XPS), and small-angle X-ray scattering (SAXS). Scanning transmission electron microscopy (STEM) and differential scanning calorimetry (DSC) demonstrated the selective incorporation of vanadium oxide within the ion-conducting POEM domains, while the oxide morphology was revealed by TEM to be a filamentous network. Cyclic voltammetry and impedance spectroscopy confirmed the preservation of the redox properties of the vanadium oxide and the ion-conductive properties of the polymer in hybrid films. Co-assembled nanocomposite films incorporating up to 34 wt % (13 vol %) vanadium oxide were flexible and semi-transparent.

Introduction

Hybrid organic/inorganic nanocomposite materials are widely being developed for drug delivery,[1] catalysis,[2] and energy storage[3] applications, among others.[4,5] To this end, microphase-separating block copolymers provide useful structure-directing agents for the in situ growth of inorganic components.[6] Exploiting the affinities of the different block components and their self-assembled morphologies, inorganic materials can be directed to grow in specific block domains, resulting in well-controlled hybrid structures.[7,8] For example, Cohen et al.[9,10] and others[11] developed various organometallic reactor schemes to synthesize metal[12,13] and semiconductor[14−16] nanophases in one domain of a block copolymer. Wiesner and co-workers employed sol−gel chemistry to grow aluminosilicates from metal alkoxide precursors within the poly(ethylene oxide) (PEO) domains of a polyisoprene-*block*-poly(ethylene oxide) block copolymer.[17]

The use of block copolymers as structure-directing agents to fabricate active lithium battery components has been shown to enhance their performance. The inherently high surface area-to-volume ratio provided by nanoscale structures facilitates ion and electron transfer, increasing rate capability.[18] In battery systems where bulk electrode diffusion is the limiting factor to performance, nanoscale systems serve to shorten diffusion lengths, translating to increased capacity utilization at high current densities. Reduced stresses from volume excursions on charge/discharge in nanostructured materials can further enhance cycle life.[19−21] Mui et al. fabricated a nanocomposite anode incorporating Au nanoparticles and carbon nanotubes as active materials within a block copolymer matrix.[22] The anode was cycled over 600 times at high rates (0.5−9 C) with little capacity fade. Bullock and Kofinas reported the synthesis of $LiMn_2O_4$ within the ion-conducting block of a copolymer.[23] The

* To whom correspondence should be addressed. E-mail: amayes@mit.edu.
† Current address: Department of Chemical Engineering, Yonsei University, 134 Shinchon-dong, Seodaemun-gu, Seoul 120-749, South Korea.

(1) Brigger, I.; Dubernet, C.; Couvreur, P. *Adv. Drug Delivery Rev.* **2002**, *54*, 631.
(2) Esumi, K.; Houdatsu, H.; Yoshimura, T. *Langmuir* **2004**, *20*, 2536.
(3) Gangopadhyay, R.; De, A. *Chem. Mater.* **2000**, *12*, 608.
(4) Park, C.; Yoon, J.; Thomas, E. L. *Polymer* **2003**, *44*, 6725.
(5) Sanchez, C.; Julian, B.; Belleville, P.; Popall, M. *J. Mater. Chem.* **2005**, *15*, 3559.
(6) Thompson, R. B.; Ginzburg, V. V.; Matsen, M. W.; Balazs, A. C. *Macromolecules* **2002**, *35*, 1060.
(7) Templin, M.; Franck, A.; Du Chesne, A.; Leist, H.; Zhang, Y.; Ulrich, R.; Schadler, V.; Wiesner, U. *Science* **1997**, *278*, 1795.
(8) Lopes, W. A.; Jaeger, H. M. *Nature* **2001**, *414*, 735.
(9) Cohen, R. E. *Curr. Opin. Solid State Mater. Sci.* **1999**, *4*, 587.
(10) Cieben, J. F.; Clay, R. T.; Sohn, B. H.; Cohen, R. E. *New J. Chem.* **1998**, *22*, 685.
(11) Sohn, B.-H.; Seo, B.-W.; Yoo, S.-I. *J. Mater. Chem.* **2002**, *12*, 2564.
(12) Boontongkong, Y.; Cohen, R. E.; Rubner, M. F. *Chem. Mater.* **2000**, *12*, 1628.
(13) Abes, J. I.; Cohen, R. E.; Ross, C. A. *Mater. Sci. Eng., C* **2003**, *23*, 641.
(14) Kane, R. S.; Cohen, R. E.; Silbey, R. *Chem. Mater.* **1996**, *8*, 1919.
(15) Joly, S.; Kane, R.; Radzilowski, L.; Wang, T. C.; Wu, A.; Cohen, R. E.; Thomas, E. L.; Rubner, M. F. *Langmuir* **2000**, *16*, 1354.
(16) Leppert, V. J.; Murali, A. K.; Risbud, S. H.; Stender, M.; Power, P. P.; Nelson, C.; Bannerjee, P.; Mayes, A. M. *Philos. Mag. B* **2002**, *82*, 1047.
(17) Ulrich, R.; Du Chesne, A.; Templin, M.; Wiesner, U. *Adv. Mater.* **1999**, *11*, 141.
(18) Patrissi, C. J.; Martin, C. R. *J. Electrochem. Soc.* **2001**, *148*, A1247.
(19) Yang, J.; Winter, M.; Besenhard, J. O. *Solid State Ionics* **1996**, *90*, 281.
(20) Winter, M.; Besenhard, J. O.; Spahr, M. E.; Novak, P. *Adv. Mater.* **1998**, *10*, 725.
(21) Wang, C.; Appleby, A. J.; Little, F. E. *J. Power Sources* **2001**, *93*, 174.
(22) Mui, S. C.; Trapa, P. E.; Huang, B.; Soo, P. P.; Lozow, M. I.; Wang, T. C.; Cohen, R. E.; Mansour, A. N.; Mukerjee, S.; Mayes, A. M.; Sadoway, D. R. *J. Electrochem. Soc.* **2002**, *149*, A1610.
(23) Bullock, S.; Kofinas, P. *J. Power Sources* **2004**, *132*, 256.

10.1021/cm060119s CCC: $33.50
Published on Web 05/16/2006

resulting nanocomposite cathode retained over 90% of its initial capacity after 300 cycles. Liu et al. produced mesoporous thin-film vanadium oxide structures using electrodeposition in the presence of block copolymer surfactants. These films showed increased capacity at high rates (125 mA·h/g at a 50 C rate) over that of the control sample.[24]

In this study, sol−gel chemistry is explored as an approach to preparing vanadium oxide active phases within the ion-conducting domains of a block copolymer. Vanadium pentoxide (V_2O_5) has been studied extensively as an insertion electrode material for lithium rechargeable batteries, due to its high energy density, ease of fabrication, and relative safety.[25−27] In addition, vanadium oxides have shown promise as optical switching materials on the basis of their electrochromic properties.[28−31] Sol−gel chemistries using vanadium alkoxide precursors produce amorphous V_2O_5 at room temperature,[32] allowing in situ oxide synthesis without degradation of the organic matrix.[33] Herein, the block copolymer poly(oligooxyethylene methacrylate)-*block*-poly(butyl methacrylate), POEM-*b*-PBMA, was chosen as a matrix for its demonstrated utility as a battery electrolyte, mechanical properties, and ease of synthesis.[34] We find that a continuous, amorphous V_2O_5 phase can be formed within the POEM domains of a POEM-*b*-PBMA copolymer (70 wt % POEM) up to weight ratios of 34%.

Experimental Section

The block copolymer POEM-*b*-PBMA with a 70:30 weight ratio of POEM to PBMA and approximately nine ethylene oxide units per POEM side chain was synthesized by atom transfer radical polymerization as described previously.[34] The polymer microphase separates into regions of ion-conducting POEM domains and mechanically stabilizing domains of PBMA. The final POEM-*b*-PBMA material had a molecular weight of 70 kg/mol and polydispersity index of 1.26, based on gel permeation chromatography calibrated with polystyrene standards.

Co-assembled nanocomposites were obtained by first dissolving 5 wt % POEM-*b*-PBMA in acetone. Varying amounts (20−60 wt %) of the precursor vanadyl triisopropoxide, $VO(OC_3H_7)_3$ ($VO(O^iPr)_3$, Gelest), were added to the polymer solution, and the resulting solutions were stirred for 30 min. To catalyze the sol−gel process, deionized water was added, maintaining the mole ratio of H_2O/V at 40:1. After stirring for 1 h the solutions were solvent cast into Teflon dishes and dried in air at room temperature under glass Petri dishes to slow the evaporation process. After air-drying for at least 48 h, films were heated under vacuum at 80 °C overnight to remove residual solvent. As the wet gel aged, film color changed from dark red to green as a result of partial reduction of V^{5+} to V^{4+}.[35]

Small-angle X-ray scattering (SAXS) experiments were carried out on a Molecular Metrology two-dimensional SAXS system with Cu Kα radiation ($\lambda = 1.542$ Å) operated at 45 kV and 0.67 mA. A 600 μm X-ray beam was provided via pinhole collimation and a fine focus filament. The sample-to-detector distance was 1.3 m, and silver behenate was used as a calibration standard. Two-dimensional data were radially averaged to produce $I(q)$ versus q plots where $I(q)$ is the scattered intensity at wavevector $q = [4\pi \sin \theta]/\lambda$ and θ is the scattering angle. All data were corrected for background scattering and plotted as log $I(q)$ versus q to better delineate the peaks.

X-ray photoelectron spectroscopy (XPS) was used to verify the valence state of the vanadium oxide phase. Experiments were performed on a Kratos Axis Ultra (Kratos Analytical, Manchester, U.K.) X-ray photoelectron spectrometer employing a monochromatic Al Kα source ($h\nu = 1486.7$ eV) and an electron takeoff angle of 90° relative to the sample plane. A survey scan (0−1100 eV binding energy range, 160 eV pass energy) and high-resolution scans of the V 2p and O 1s peaks (10 eV pass energy) were run for each sample.

Wide-angle X-ray scattering (WAXS) experiments were carried out on a Rigaku Rotaflex 18 kW rotating anode X-ray generator with Cu Kα radiation operated at 60 kV and 300 mA. The 2θ range was from 5 to 55° with a scanning speed of 1°/min and sample-to-detector distance of 185 mm. Data were acquired in transmission mode to obtain a stronger signal.

Microstructural characterization of the nanocomposite films was carried out using transmission electron microscopy (TEM; JEOL 2010 CX) in bright field mode at 200 keV. The samples were prepared by cryomicrotoming ∼50 nm sections using a diamond knife, placing the sections on copper grids, and coating them with ∼15 nm of carbon through thermal evaporation. Some polymer samples with and without vanadium oxide were stained with ruthenium tetraoxide for image contrast. Scanning transmission electron microscopy (STEM, VG) was performed on the same samples for chemical mapping of vanadium within the polymer.

Thermogravimetric analysis (TGA) was used to determine the vanadium oxide content of nanocomposite films after solvent evaporation. TGA (model Q50, TA Instruments, Inc.) was performed under a nitrogen atmosphere using a heating rate of 20°/min and a temperature range of 30−600 °C. Differential scanning calorimetry (DSC) was performed on a DSC Q100 (TA Instruments, Inc.). Samples were sealed in Al pans and heated at a rate of 20 °C/min in a flowing atmosphere of nitrogen (50 mL/min). The temperature range for DSC measurements was −100 to +90 °C, and the data were taken upon heating.

The nanocomposite films were characterized by electrochemical methods. The redox behavior of vanadium oxide in the nanocomposite was compared to that of vanadium oxide alone by cyclic voltammetry (CV) in a three-electrode cell. The electrolyte consisted of 1 M $LiClO_4$ in propylene carbonate electrolyte solution. The working electrode was made by spin coating the vanadium oxide sol with and without POEM-*b*-PBMA onto indium tin oxide-coated glass substrates. Films were subsequently heated under vacuum at 80 °C overnight. The reference electrode was a glass tube closed at one end containing a silver wire immersed in a solution of acetonitrile saturated with $AgNO_3$. A frit at the bottom of the tube enabled electrical contact with the electrolyte in the main chamber. A platinum foil served as the counter electrode. The potential was swept from −1.0 to 1.5 V versus Ag/Ag^+ at 50 mV/s using a

(24) Liu, P.; Lee, S.-E.; Tracy, C. E.; Yan, Y.; Turner, J. A. *Adv. Mater.* **2002**, *14*, 27.
(25) Chaput, F.; Dunn, B.; Fuqua, P.; Salloux, K. *J. Non-Cryst. Solids* **1995**, *188*, 11.
(26) Dong, W.; Rolison, D. R.; Dunn, B. *Electrochem. Solid−State Lett.* **2000**, *3*, 457.
(27) Sudant, G.; Baudrin, E.; Dunn, B.; Tarascon, J. M. *J. Electrochem. Soc.* **2004**, *151*, A666.
(28) Wang, Z.; Chen, J.; Hu, X. *Thin Solid Films* **2000**, *375*, 238.
(29) Ozer, N. *Thin Solid Films* **1997**, *305*, 80.
(30) Livage, J. *Coord. Chem. Rev.* **1999**, *190−192*, 391.
(31) Takahashi, K.; Wang, Y.; Cao, G. *Appl. Phys. Lett.* **2005**, *86*, 053102.
(32) Livage, J. *Solid State Ionics* **1992**, *50*, 307.
(33) Simon, P. F. W.; Ulrich, R.; Spiess, H. W.; Wiesner, U. *Chem. Mater.* **2001**, *13*, 3464.
(34) Trapa, P. E.; Huang, B.; Won, Y.-Y.; Sadoway, D. R.; Mayes, A. M. *Electrochem. Solid−State Lett.* **2002**, *5*, A85.
(35) Tang, P.; Sakamoto, J. S.; Baudrin, E.; Dunn, B. *J. Non-Cryst. Solids* **2004**, *350*, 67.

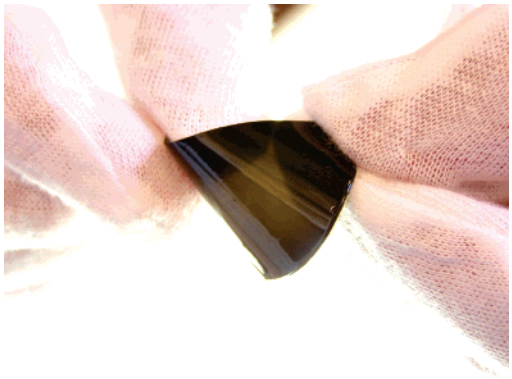

Figure 1. POEM-*b*-PBMA film incorporating 18 wt % vanadium oxide (from 30 wt % precursor) grown in situ by sol−gel chemistry.

potentiostat (Solartron 1287, Solartron Analytical, Oak Ridge, TN) controlled by a PC running CorrWare (Scribner Associates, Inc., Southern Pines, NC).

In addition, the conductivity of the block copolymer with and without vanadium oxide was measured by impedance spectroscopy using a frequency response analyzer (Solartron 1255, Solartron Analytical, Oak Ridge, TN), coupled to a potentiostat (Solartron 1287, Solartron Analytical, Oak Ridge, TN) and controlled by a PC running commercially available software (Zplot, Scribner Associates, Inc., Southern Pines, NC). The test fixture consisted of two blocking electrodes made of stainless steel; a Teflon washer of known diameter fixed the specimen area. The thickness of the sample was measured using a micrometer before and after measurement to verify its consistency throughout the experiment. Polymer films doped with $LiCF_3SO_3$ at a Li:EO ratio of 1:20 were cast from tetrahydrofuran (THF) and dried under vacuum overnight at room temperature. For nanocomposite films, a solution of $LiCF_3SO_3$ in THF was added dropwise to a film of known thickness and area containing 25 wt % V_2O_5 until a Li/EO ratio of 1:20 was obtained. The film was dried overnight under vacuum at room temperature.

Results and Discussion

Solution cast films of POEM-*b*-PBMA incorporating the product vanadium oxide from in situ sol−gel synthesis were semi-transparent and flexible for precursor contents < 60 wt %. Figure 1 shows a film sample prepared from a 30 wt % $VO(O^iPr)_3$ precursor solution. The semi-transparent nature of the film suggests the absence of macrophase separation of the organic and inorganic phases and provides a first indication that the vanadium oxide grows confined within the domains of the microphase-separated block copolymer. As shown in Figure 2, the weight fraction of the vanadium oxide inorganic phase incorporated into the polymer, as determined by TGA, varied linearly with precursor concentration in the casting solution.

Further evidence for nanodomain confinement of the oxide is given in SAXS patterns taken on POEM-*b*-PBMA incorporating increasing weight fractions of vanadium oxide, as seen in Figure 3 (data are offset for clarity). The SAXS pattern for neat POEM-*b*-PBMA is consistent with that of a material possessing a cylindrical morphology with a domain periodicity, *d*, of ~35 nm. The peak/shoulder visible at $q \sim 0.076$ nm^{-1} is attributed to the beamstop of the instrument and was deconvolved from the primary reflection in performing peak fitting of the scattering maximum. The shift to lower *q* values of the observed maximum in SAXS

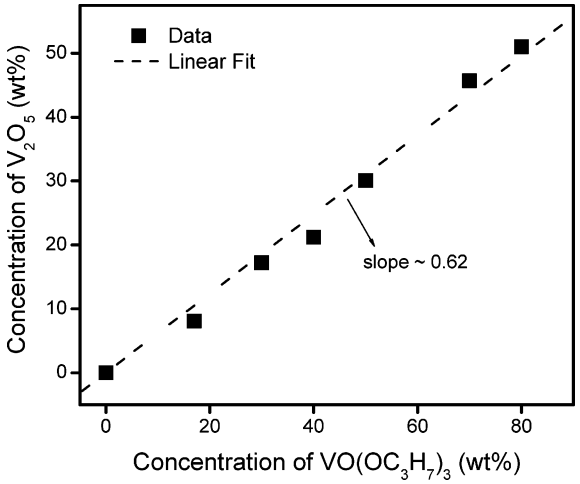

Figure 2. Weight fraction of vanadium oxide determined from TGA as a function of precursor concentration for nanocomposite films.

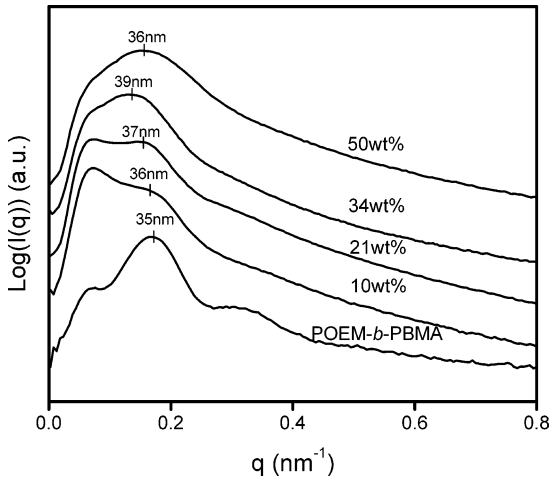

Figure 3. SAXS patterns for neat POEM-*b*-PBMA copolymer and nanocomposite films with vanadium oxide weight percentages as indicated.

patterns from nanocomposite films indicates an increase in the period as vanadium oxide content increases. For an oxide volume fraction of 34 wt % (13 vol %), *d* increases by 11% over that of the neat copolymer. Additionally, the second-order reflection was absent for nanocomposite films, suggesting a change in morphology and/or loss of long range order. At higher inorganic loadings, the peak of the SAXS trace shifts back toward higher *q* (lower *d*) suggesting partial macrophase separation of the oxide phase.

Figure 4 shows TEM micrographs of the POEM-*b*-PBMA matrix (a), a nanocomposite film incorporating 24 wt % vanadium oxide (b), and a film incorporating 50 wt % oxide (c). In Figure 4a, preferential staining of POEM domains by ruthenium tetraoxide provides contrast between the POEM (dark) and PBMA (light) domains and is consistent with the cylindrical morphology indicated in the SAXS pattern for the neat polymer. $VO(O^iPr)_3$ and its hydrolysis products are expected to preferentially incorporate into the POEM block as a result of its hydrophilic PEO side chains and ability for hydrogen bonding.[36] In parts b and c, the polymer is unstained so that POEM and PBMA are indistinguishable.

(36) De Paul, S. M.; Zwanziger, J. W.; Ulrich, R.; Wiesner, U.; Spiess, H. W. *J. Am. Chem. Soc.* **1999**, *121*, 5727.

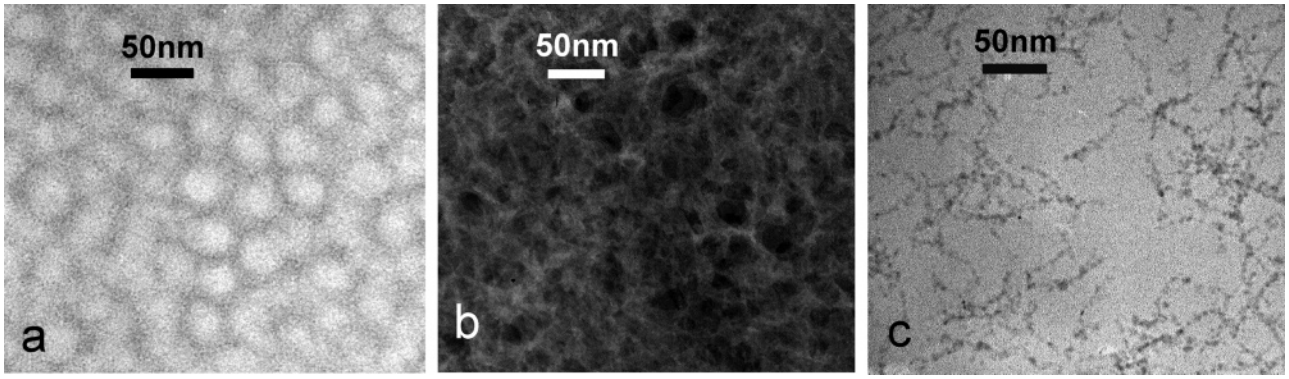

Figure 4. TEM micrographs of (a) POEM-*b*-PBMA (70:30) stained with RuO_4; (b) POEM-*b*-PBMA containing 24 wt % V_2O_5; and (c) POEM-*b*-PBMA containing 50 wt % V_2O_5.

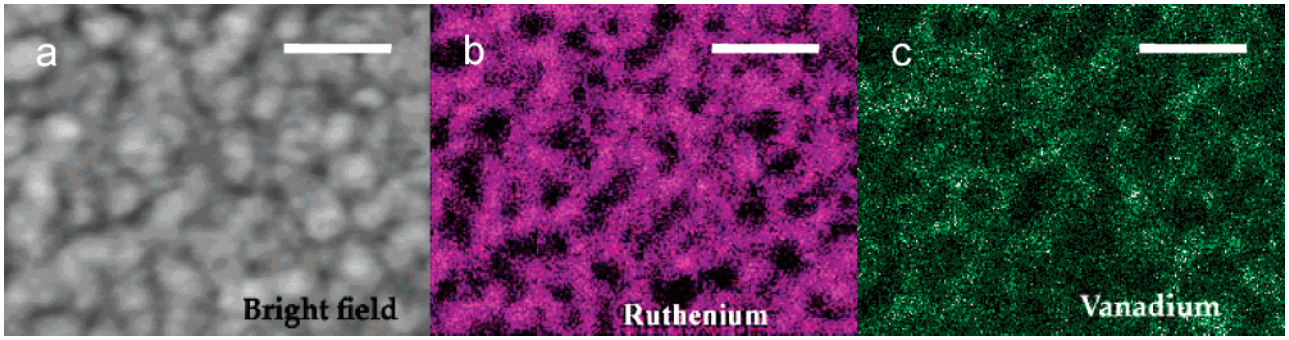

Figure 5. STEM micrographs of POEM-*b*-PBMA containing 24 wt % vanadium oxide: (a) bright field stained with RuO_4; (b) ruthenium chemical map; and (c) vanadium chemical map (scale bar = 90 nm).

Figure 4b, shown in dark field mode to provide better contrast, is representative of systems containing 10−34 wt % inorganic phase. The vanadium oxide phase (light) is seen to form a filamentous network, akin to the ribbonlike morphologies reported in the literature for sol−gel synthesized V_2O_5.[37] Regions devoid of vanadium oxide are visible on the same size scale as the PBMA domains of the neat polymer. However, the structure of the voids is inconsistent with that of cylinder microdomains, indicating a change in morphology with the addition of vanadium oxide as noted from SAXS patterns. Transformation to spherical PBMA domains due to the increase in effective volume of POEM domains might be expected; alternatively, a bicontinuous network could yield an oxide microstructure similar to that seen in Figure 4b. At still higher oxide contents, macrophase separation was observed, consistent with SAXS results. In Figure 4c, taken from a sample containing 50 wt % inorganic phase, large regions devoid of vanadium oxide are evidence of macrophase phase separation between the inorganic phase and the copolymer.

Verification of vanadium oxide confinement to the POEM domains for lower oxide contents was obtained by chemically mapping ruthenium and vanadium in a RuO_4 stained sample using STEM. Figure 5a shows the bright field image of a RuO_4-stained film incorporating 24 wt % vanadium oxide. Figure 5b,c displays the distribution of ruthenium and vanadium, respectively. The strong similarities in the spatial distribution patterns of these two figures confirm the colocation of vanadium oxide and POEM. These micrographs also appear more consistent with interconnected PBMA domains than isolated PBMA spheres.

DSC measurements provided further evidence for the confinement of vanadium oxide to the POEM domains. DSC traces from the nanocomposites show that the T_g value of the PBMA domains remains constant at 20 °C, while the T_g value of the POEM domain increases with the addition of the vanadium oxide. The POEM T_g value is observed to shift from −69 °C for the neat copolymer to −60 °C for 24 wt % oxide incorporation. This can be explained by the interaction of the vanadium oxide with the ether oxygen groups of POEM, which serves to reduce the chain mobility.

The formation of amorphous V_2O_5 through the sol−gel process was demonstrated by XPS (Figure 6) and WAXS (Figure 7). Figure 6 shows the XPS V 2p high-resolution spectrum for sol−gel synthesized vanadium oxide in the absence of the copolymer (a), along with that from a nanocomposite sample prepared by in situ hydrolysis (b). The results are presented after Shirley background subtraction. The V 2p peaks at 518 eV ($2p_{1/2}$) and 525.5 eV ($2p_{3/2}$) observed in the pure vanadium oxide sample (Figure 6a) strongly resemble the spectrum for V_2O_5 previously published.[38] The nanocomposite film similarly shows a predominance of these peaks in the high-resolution 2p spectrum (Figure 6b). In addition, both spectra exhibit shoulders at lower binding energies characteristic of the V^{4+} state, consistent with the color change observed in the film preparation. From the relative intensities of the V^{4+} and V^{5+}

(37) Dunn, B.; Farrington, G. C.; Katz, B. *Solid State Ionics* **1994**, *70/71*.

(38) Demeter, M.; Neumann, M.; Reichelt, W. *Surf. Sci.* **2000**, *454−456*, 41.

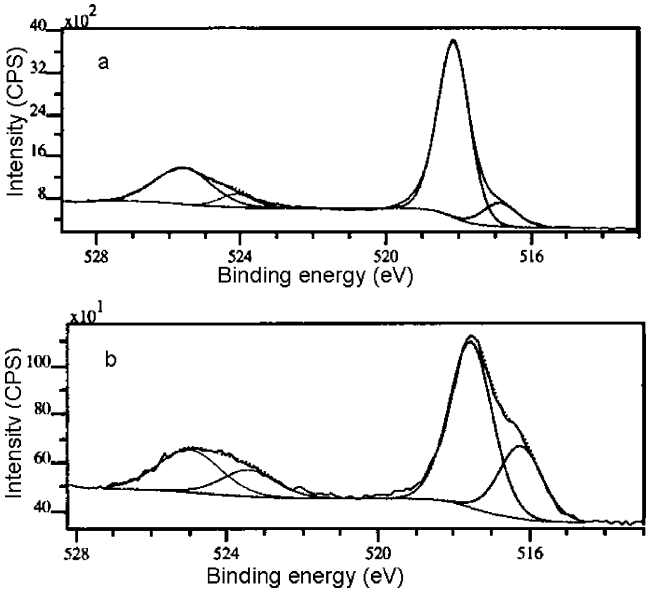

Figure 6. XPS high-resolution spectra of the V 2p peak for (a) neat vanadium oxide prepared by sol−gel synthesis and (b) vanadium oxide grown within the block copolymer.

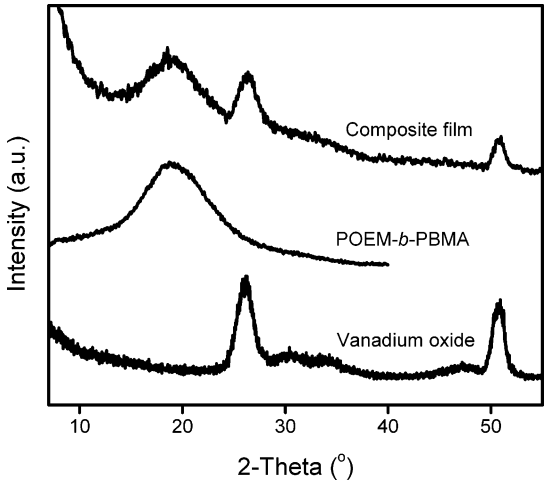

Figure 7. WAXS patterns for neat POEM-*b*-PBMA (70:30), neat amorphous vanadium oxide from the sol−gel process, and the nanocomposite film.

contributions, ∼88% and 70% of the vanadium is in a 5+ state for the neat oxide and nanocomposite, respectively. From the low-resolution XPS spectra, the V/O mole ratio for the neat oxide was 3.1:1, indicating 80% V_2O_5 stoichiometry. The larger V^{4+} content for the nanocomposite samples may indicate incomplete hydrolysis of the vanadium oxide or participation of the polymer in the gelation and condensation process.

WAXS data contained in Figure 7 depict patterns from neat POEM-*b*-PBMA, neat V_2O_5, and a nanocomposite film incorporating 24 wt % V_2O_5. The WAXS data reveal the V_2O_5 to be amorphous, with short range order peaks at 26 and 51°, in agreement with values reported in the literature.[27] The WAXS pattern for POEM-*b*-PBMA exhibits a dominant short range order peak at ∼18° corresponding to the van der Waals distance between nonbonded atoms (C−C and C−O).[39] The XRD pattern of the composite film is a direct superposition of the patterns from its components. The

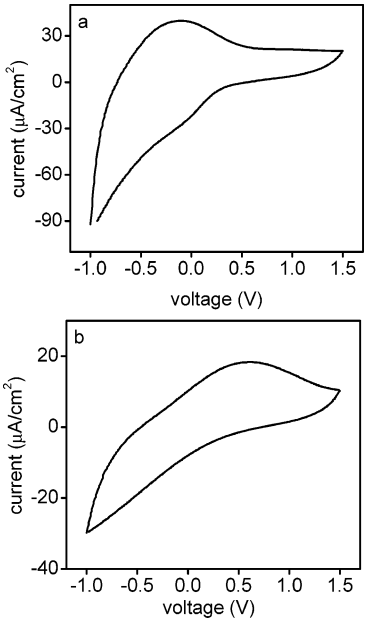

Figure 8. Cyclic voltammograms for (a) vanadium oxide and (b) nanocomposite spin coated films in $LiClO_4$/propylene carbonate electrolyte. Swept from −1.0 to +1.5 V at 50 mV/s vs Ag/Ag^+.

combined XPS, WAXS, and DSC data indicate only slight modification to the oxide and polymer as a consequence of co-assembly.

The redox activity of V_2O_5 and ion-conducting properties of POEM for use in battery electrodes or electrochromic devices were substantially preserved in the nanocomposite materials. The CV curves for the vanadium oxide film with and without POEM-*b*-PBMA are shown in Figure 8a,b, respectively. The vanadium oxide film alone is characterized by one set of corresponding redox peaks reflecting intercalation/deintercalation of Li^+ into/from the V_2O_5 structure. The mixed oxide/polymer electrode exhibited the same peaks, although somewhat broadened and separated by a slightly larger potential, owing to the increased resistance of the polymer matrix as compared to that of the liquid electrolyte alone. Still, the peaks in the voltammogram of the nanocomposite film are the electrical signature of lithiation and delithiation of the vanadium oxide.

The value of the electrical conductivity of POEM-*b*-PBMA doped with $LiCF_3SO_3$ at an Li/EO ratio of 1:20 was measured to be 3×10^{-6} S/cm at room temperature which agrees with previous characterizations of this material as a solid electrolyte.[34] When the identical polymer was loaded with vanadium oxide to a level of 25 wt % and doped with $LiCF_3SO_3$ (Li/EO ratio 1:20), the maximum room-temperature conductivity was determined to be 1.8×10^{-6} S/cm. The slightly lower value of the conductivity of the composite film compared to that of the neat polymer electrolyte can be attributed to the lower conductivity of V_2O_5. In addition, interaction between the oxide and POEM, as evidenced by the increase in T_g, retards segmental motion in the polymer.

(39) Miller, R. L.; Boyer, R. F. *J. Polym. Sci., Part B: Polym. Phys.* **1984**, *22*, 2021.

Conclusions

Block copolymer/V_2O_5 nanocomposite films were prepared via sol−gel synthesis from vanadium alkoxide precursor in a microphase-separating POEM-*b*-PBMA matrix. WAXS and XPS confirm the formation of amorphous V_2O_5 while SAXS, STEM, and DSC indicate its selective incorporation in the ion conductive POEM domains. CV and impedance spectroscopy indicate that the electrochemical properties of the V_2O_5 and POEM-*b*-PBMA are substantially preserved in the nanocomposite film. These hybrid materials have possible application as electrodes for lithium rechargeable batteries or electrochromic devices. Work in progress indicates that the structure-directing properties of microphase-separating copolymers can also be exploited in constructing electronically conductive pathways serving as connections to the lithium-active vanadium oxide domains.

Acknowledgment. This work was sponsored by the Office of Naval Research under Contract Nos. N00014-02-1-0226 and N00014-05-1-0056 and in part by the MIT MRSEC Program of the National Science Foundation under Award No. DMR-0213282. J.H.K. acknowledges the partial support of the Postdoctoral Fellowship Program of Korea Science & Engineering Foundation (KOSEF). The authors gratefully acknowledge Dr. Tony Garrett-Reed for his assistance with the STEM work and Ms. Libby Shaw for her assistance with the XPS.

CM060119S